*eXPRESS Polymer Letters Vol.10, No.5 (2016) 381–393*
*Available online at www.expresspolymlett.com*
*DOI: 10.3144/expresspolymlett.2016.36*

# Effect of halloysite on structure and properties of melt-drawn PCL/PLA microfibrillar composites

*I. Kelnar[1*], J. Kratochvíl[1], I. Fortelný[1], L. Kaprálková[1], A. Zhigunov[1], V. Khunová[2], M. Nevoralová[1]*

[1]Institute of Macromolecular Chemistry, Academy of Sciences of the Czech Republic, Heyrovského nám. 2, 162 06 Praha, Czech Republic
[2]The Slovak University of Technology, Faculty of Chemical and Food Technology, Radlinského 9, 812 37 Bratislava, Slovakia

*Received 30 September 2015; accepted in revised form 7 December 2015*

**Abstract.** The study deals with the modification of mechanical properties of poly (ε-caprolactone) (PCL)/poly(lactic acid) (PLA) system using the microfibrillar composite (MFC) concept. As the *in-situ* formation of PLA fibrils by melt drawing was impossible due to flow instability during extrusion, the system was modified by adding halloysite nanotubes (HNT) using different mixing protocols. The resulting favourable effect on the rheological parameters of the components allowed successful melt drawing. Consequently, PLA fibrils formation combined with the reinforcement of components by HNT and increased PLA crystallinity lead to a biocompatible and biodegradable material with good performance suitable for a broad range of applications. The best results, comparable with analogous MFC modified with layered silicate (oMMT), have been achieved at a relatively low content of HNT of 3%, in spite of its lower reinforcing ability in a single nanocomposite. This indicates that modifying MFC by HNT, including fibrils and interface parameters, is more complex in comparison with the undrawn system.

***Keywords:*** *mechanical properties, poly(ε-caprolactone), poly(lactic acid), microfibrillar composites, halloysite nanotubes*

## 1. Introduction

PCL is an important biodegradable polymer with favourable functional parameters for biomedical, packaging, and other applications [1]. In spite of its semicrystalline character and relatively high content of crystalline phase, mostly over 50%, its poorly organized crystalline structure in combination with low glass transition temperature ($T_g$) are the main reasons of relatively poor mechanical performance. As a result, low yield stress, stiffness, and high ductile deformation under ambient conditions limit the range of PCL applications. The purpose of numerous modifications is, in particular, higher yield stress and modulus [1]; advantageous modifications are those preserving biodegradability, for instance blending with more rigid polyesters, mostly PLA [2–5]. As a consequence, a broad range of materials with balanced and tailored mechanical performance can be obtained. The mostly applied PLLA containing 2–4% D-isomer has low compatibility with PCL [5]; therefore, various compatibilizing techniques [6, 7] must be applied. In this area, application of various nanofillers (NF) leading to simultaneous reinforcement, compatibilization, and improvement of other material parameters may also be beneficial [8–12]. Recently, halloysite nanotubes have been successfully applied to modification of PLA [13, 14] and PCL [15, 16]; their advantage is dispersion even without organophilization in these polar polymers. In some cases, suitable modifications can enhance HNT efficiency [17, 18]. However, the evaluation of the structure-directing potential of HNT in polymer

*Corresponding author, e-mail: kelnar@imc.cas.cz

blends [19–23] is in its infancy stage, especially in comparison with that of oMMT [24–27].

Although the application of PLA and other high performance polyesters in the form of short reinforcing fibres [28, 29] in polymer-polymer composites could be a radical alternative to the use PCL/PLA blends, a significant limitation of this method is the difficult dispersion of compliant fibres in the polymer matrix and their relatively poor adhesion to it [30]. An advantageous method to prepare these polymer fibre-reinforced materials is the formation of microfibrillar composites [31]. This method is based on melt- or cold drawing of a polymer blend with a rigid and strong dispersed phase which should be semicrystalline with a melting point exceeding that of the matrix, e.g. the HDPE/PA6 combination [32]. In this case, subsequent processing below the melting point of the dispersed phase may lead only to isotropization of the matrix with preserved fibrils. An advantage of such short-fibre composite is efficient dispersion and bonding of *in-situ* formed reinforcement [33].

A suitable polymer pair for MFC is a combination of biodegradable linear polyesters, like the PCL/PLA blend. Friedrich *et al*. [34] and Kimble *et al.* [35] prepared PLA/ poly(glycolic acid) melt-drawn MFC for medical application. The recently reported PLA/ poly(butylene succinate) system melt-drawn with *in-situ* formed PLA short fibres could not be processed using thermoplastic processing technique due to the similarity of the components' melting points [36]. The MFC concept was also applied to PLA microfibrils preparation [37]. Some other systems of drawn fibres based on the blend of these polyesters were reported by others [38, 39]. The reason that the attractive PCL/PLA blend-based MFC has not been reported lies probably in the fact that, according to our experiments, the commercial PCL/PLA combinations cannot be successfully drawn due to unfavourable rheological parameters and thus to flow instability during extrusion, i.e. variation in the extrudate cross dimension [40]. We have successfully prepared this MFC in the case of clay addition that favourably affects extrusion stability and thus melt drawing [40]. Moreover, the nanofiller eliminates the main shortcoming of MFC, i.e. the relatively poor mechanical performance and dimensional stability due to the low mechanical parameters of polymer fibrils [41]. Our previous work indicates that the effect of NF on drawn systems is relatively complex, which may lead even to the deterioration of mechanical properties [42]. The present work deals with the modification of PCL/PLA MFC using halloysite, a nanofiller with reported high reinforcing ability and fair dispersion without modifications in polar polymers like polyesters.

## 2. Experimental

### 2.1. Materials

Poly(lactic acid) (PLA) Ingeo 2002D (Nature Works, Minnetonka, USA) with the D-isomer content of 4.3%, $M_w$ $2.53 \cdot 10^5$ g·mol$^{-1}$, melt flow rate 6 g/10 min (190 °C/2.16 kg), and density 1.24 g·cm$^{-3}$. Poly(ε-caprolactone) (PCL) CAPA 6800 (Perstorp, Sweden) $M_n$ $8 \cdot 10^4$ g·mol$^{-1}$, density 1.145 g·cm$^{-3}$. Halloysite nanotubes (HNT) were purchased from Sigma Aldrich (USA).

### 2.2. MFC preparation

Prior to mixing, PCL, PLA, and HNT were dried at 45, 85, and 70 °C, respectively, in a vacuum oven for 12 h. Mixing was carried out in a co-rotating segmented twin-screw extruder ($L/D$ 40) Brabender TSE 20 (Brabender GmbH, Duisburg, Germany) at 400 rpm, and temperatures of the respective zones (from feeding to die) of 170, 170, 170, 170, 175, and 180 °C. The extruded bristle with the PCL/PLA 80/20 w/w composition was melt-drawn using an adjustable take-up device. The draw ratio (DR) is the ratio between the velocity of the take-up rolls and the initial velocity of the extruded bristle; DR 5 and 6 were mostly used. Besides the one-step addition of all components (with 3 phr HNT), the pre-blends of PCL with 3% HNT and PLA with 3% HNT were also used. The PCL pre-blend was mixed using temperatures 135 °C in all zones, the PLA pre-blend was mixed using temperature profile 185, 190,190, 190, 190, and 190 °C. Dog-bone specimens (gauge length 40 mm) were injected in a laboratory micro-injection moulding machine (DSM). The barrel and mould temperatures were 137 and 30 °C, respectively.

### 2.3. Testing

Tensile tests were carried out using an Instron 5800 (Instron, UK) apparatus at 22 °C and crosshead speed of 20 mm/min. At least eight specimens were tested for each sample. Young's modulus ($E$), maximum stress ($\sigma_m$), and elongation at break ($\varepsilon_b$) were evaluated; the corresponding variation coefficients did not exceed 10, 2 and 20%, respectively.

Tensile impact strength, $a_t$, was measured on one-side notched specimens using a CEAST Resil impact junior hammer (CEAST S.p.A., Torino, Italy) with an energy of 4 J (variation coefficient 10–15%). The reported values are averages of twelve individual measurements. Dynamic mechanical analysis (DMA) was performed in single-cantilever mode using a DMA DX04T (RMI, Pardubice, Czech Republic) apparatus at 1 Hz and heating rate of 1 °C/min from –120 to 250 °C.

The differential scanning calorimetry (DSC) analysis was carried out using a Perkin-Elmer 8500 DSC (Perkin Elmer, Waltham, MA, USA) apparatus. Samples of 5–10 mg were heated from 0 to 200 °C at the heating rate of 10 °C/min. The melting temperature $T_m$ was identified as the melting endotherm maximum. The crystallinity was calculated from the respective peak areas using the Perkin-Elmer software and the values 139.5 and 93.1 J/g for the heat of melting of 100%-crystalline PCL and PLA, respectively.

### 2.4. Characterization of structure

The structure of drawn and undrawn samples was examined using scanning electron microscopy (SEM) with a Quanta 200 FEG (FEI, Czech republic) microscope. The injection-moulded specimens of the undrawn blends were broken under liquid nitrogen. Because of impossibility of the separation of PLA fibrils due to chemical similarity of both polyesters, the drawn bristle samples were broken under liquid nitrogen in parallel direction with respect to their long axis. The PLA phase was etched using 20% NaOH at room temperature for 30 min.The size of the dispersed PLA particles was investigated by a MINI MOP image analyzer (Kontron Co., Germany). At least 200 particles were evaluated in each sample. For the transmission electron microscope Tecnai G2 Spirit (FEI, Czech republic) observations, ultrathin (60 nm) sections were prepared under liquid nitrogen using an Ultracut UCT (Leica Mikrosysteme GmbH, Austria) ultramicrotome.

Wide-angle X-ray Scattering (WAXS) and Small-angle X-ray scattering (SAXS) experiments were performed using a pinhole camera (Molecular Metrology System, Rigaku, Japan) attached to a microfocused X-ray beam generator (Osmic MicroMax 002, Rigaku) operating at 45 kV and 0.66 mA (30 W). The camera was equipped with an interchangeable Imaging Plate 23×25 cm (Fujifilm). For WAXS, the sample-to-detector distance was approximately 24 cm and experimental setup covered the momentum transfer ($q$) range of 0.4–3.5 Å$^{-1}$. While $q = (4\pi/\lambda)\sin\theta$, where $\lambda = 1.54$ Å is the wavelength and $2\theta$ is the scattering angle. Calibrations of the centre and sample-to-detector distance were made using Si powder. To cover the SAXS range, the sample-to-detector distance was set to 390 cm. Covered $q$-range was 0.008–0.26 Å$^{-1}$. Calibrations of the centre and sample-to-detector distance were made using Ag-behenate. For both WAXS and SAXS, one-dimensional intensity profiles $I(q)$ were circularly averaged from the two-dimensional scattering patterns. The data were deconvoluted into peaks using Fityk (A curve fitting and data analyzing program) [43].

Crystallinity was determined by the division of the area of crystal peaks by the total area. Crystal molecular orientation was determined by azimuthal integration of the strongest (110) reflection.

### 2.5. Rheological characterization

Rheological characterization was conducted using an ARES apparatus (Rheometric Scientific, Piscataway, NJ) with the parallel-plate geometry at 137 and 170 °C using an oscillatory shear deformation at frequency range 0.1–100 rad/s. The amplitude of oscillation was 3%, i.e. within the range of linear viscoelasticity of all studied materials.

## 3. Results and discussion

### 3.1. Effect of HNT on structure of undrawn blend and related MFC

Figure 1 and Table 1 show a slight reduction of the size of PLA inclusions in the PCL/PLA blend from ~0.9 μm in the HNT-free blend to ~0.5 μm with 5% HNT addition. This corresponds to well-known structure-directing effect of nanofillers, but the 'compatibilizing' effect is less marked in comparison with layered silicates [40]; more marked decrease in particle size occurs with relatively high 5% HNT content. In addition to reduced average diameter, the structure is more polydisperse (Figure 1b). Crucial role of HNT consists mainly in the improvement of extrusion stability as a result of a change in the rheological parameters (see below), which allows melt drawing of the extruded bristle and thus *in-situ* formation of the PLA fibrils. The structure and approximate dimensions of fibrils are obvious from Figure 2, the aspect ratio (AR) is ~12. Due to the comparable diameter of fibrils and dispersed particles in

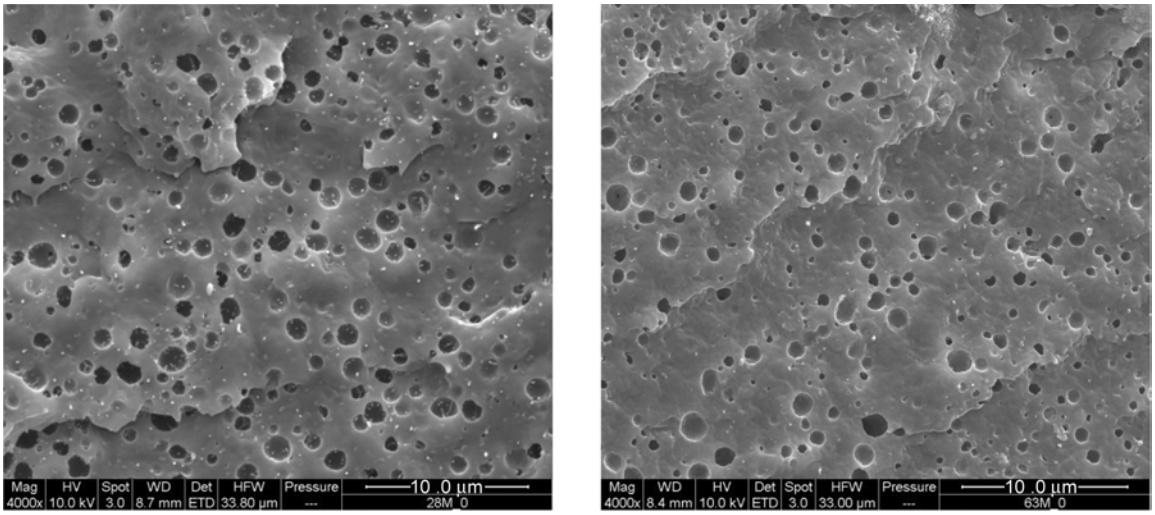


a) b)

**Figure 1.** SEM images of a) undrawn injection moulded PCL/PLA 80/20 system; b) undrawn injection moulded PCL/PLA/HNT 80/20/3 blend (one-step prepared)

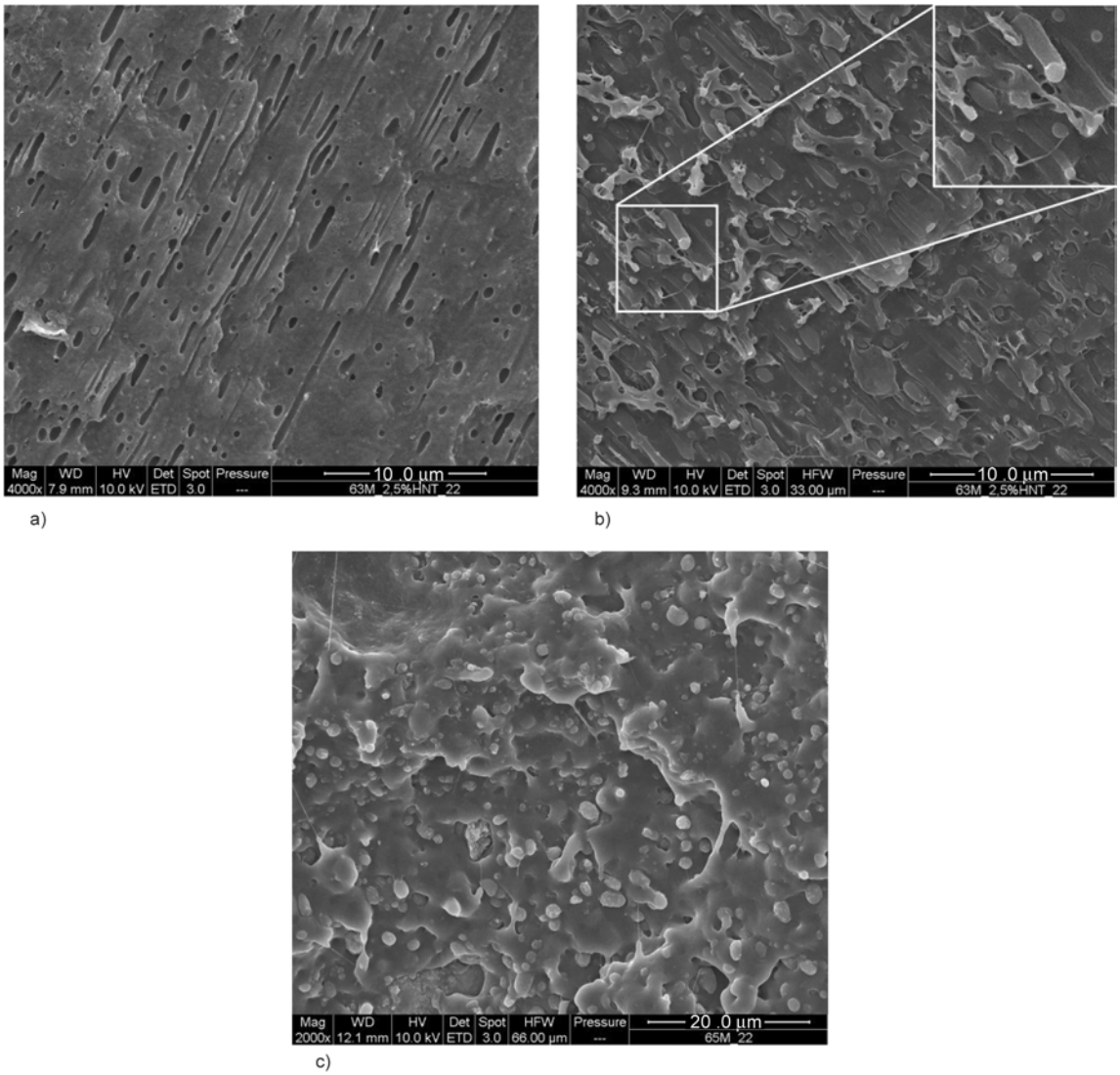


a) b)

c)

**Figure 2.** SEM images of a) etched and b) unetched melt drawn bristle (sample broken parallel to draw direction) of PCL/PLA/HNT 80/20/3 system (draw ratio = 6); c) fracture surface of the same injection moulded MFC sample

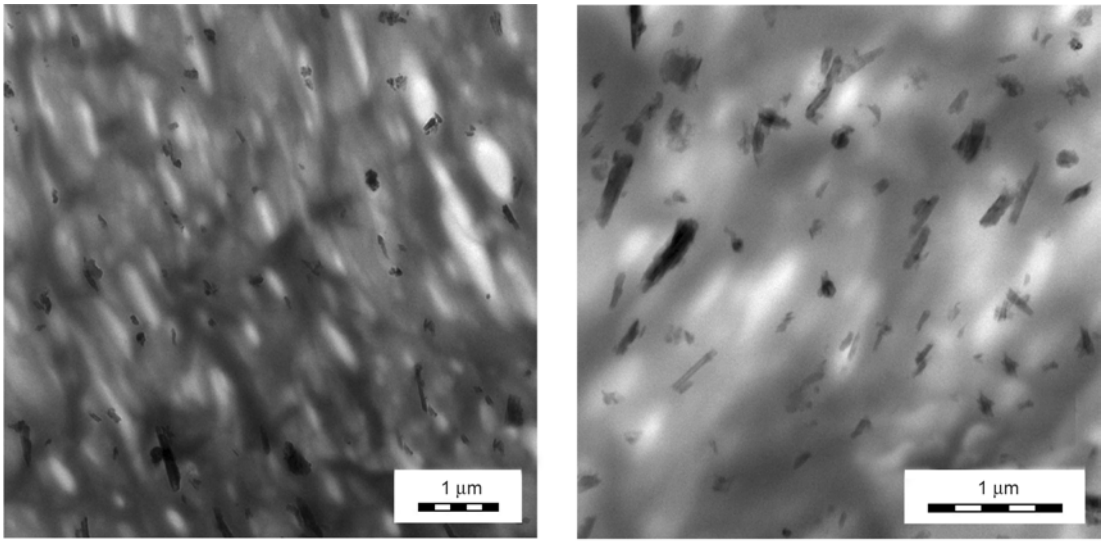


**Figure 3.** TEM of melt-drawn bristle, sample microtomed parallel to draw direction a) PCL/PLA/HNT 80/20/3, b) another place, higher magnification

**Table 1.** Effect of HNT on PLA inclusion size, one-step prepared samples

| Composition Parts by wt. | Particle diameter [µm] Undrawn sample | Fibril diameter [µm] Draw ratio 6 |
|---|---|---|
| PCL/PLA 80/20 | 0.90 | – |
| PCL/PLA/HNT 80/20/3 | 0.83 | 0.57 |
| PCL/PLA/HNT 80/20/5 | 0.50 | 0.51 |

the undrawn blend (Table 1) and thus much larger volume of fibrils, significant coalescence of PLA inclusions takes place in the course of melt drawing, in agreement with other works [44, 45]. As it is impossible to prepare HNT-free MFC, we cannot consider the possible effect of the nanofiller on coalescence, as found in clay-containing MFC based on the HDPE/PA6 combination [42]. From Figures 2 it is also apparent that diameters of the PLA fibrils in the drawn bristle and injection moulded sample are comparable. TEM images in Figure 3 show light PLA fibrils in a dark grey PCL matrix. Black HNT and their aggregates are localized predominantly in the PCL matrix and at the interface. This structure was achieved mainly in the case of simultaneous addition of all components, which leads to the most efficient drawing. In the case of other mixing protocols, pre-blending of HNT in the PLA component did not lead to successful drawing, similarly to analogous clay-containing system [40]; whereas only limited drawing is different from clay-modified MFC in the case of pre-blending of HNT with PCL. In both cases, successful drawing is possible with further simultaneous addition of HNT. As final HNT localization is similar in all the mentioned drawn systems, important factor influencing fibrils formation is HNT migration between components in the course of extrusion and drawing [42]. We suppose initial localization in the earlier melting PCL with subsequent migration to later melting PLA. This may lead to higher interfacial HNT localization in the course of drawing, which may affect attractive forces between coalescing particles [46].

### 3.2. Dynamic mechanical analysis (DMA)

Temperature dependence of loss modulus indicates negligible increase of glass transition temperature ($T_g$) of single PCL (~1.5 °C, Figure 4a) and PLA (~2 °C, Figure 4b) due to the presence of 3% HNT. This is probably a result of compensation of two effects – usual increase in $T_g$ by added nanofillers, as frequently mentioned in the literature [47], and higher chain mobility caused by increased free volume in the case of anisotropic nanofillers with length exceeding the typical gyration radii of polymer chains [48, 49].

In the PCL/PLA/HNT undrawn blend (Figure 4c), the negligible changes in $T_g$ (~2 °C increase of PCL and ~1 °C decrease for PLA) confirm practically no impact on compatibility in accordance with very low 'compatibilizing' effect of HNT (Figure 1, Table 1) From Figure 4c it is further obvious that drawing practically does not affect $T_g$ of the PCL matrix in the analogous MFC system, whereas slightly higher $T_g$ of PLA fibrils undoubtedly caused by drawing was found [42].

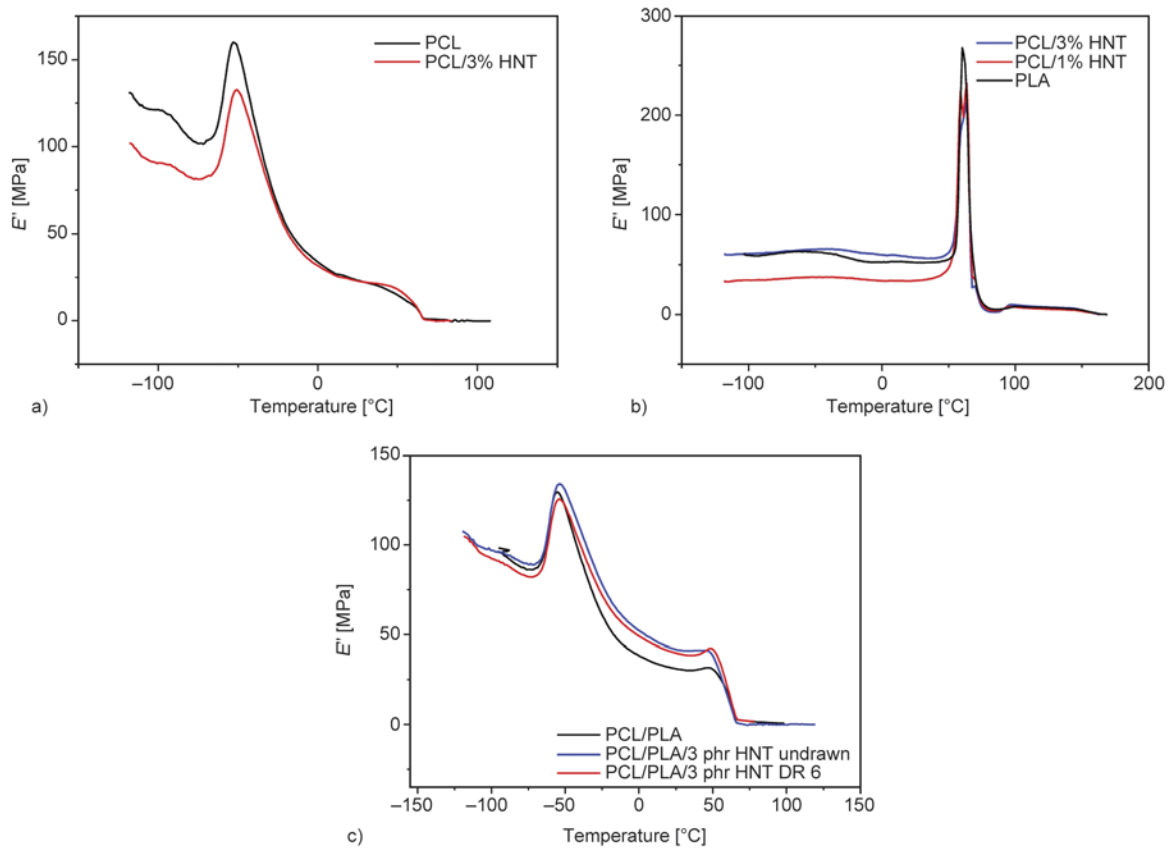


**Figure 4.** Temperature dependence of loss modulus a) PCL/HNT, b) PLA/HNT, c) PCL/PLA/HNT

### 3.3. Effect of HNT and drawing on crystallinity

*WAXS-SAXS analysis*

Figure 5 shows the typical two-dimensional WAXS pattern. The brightest circle corresponds to (110) PCL peak, but the behaviour is anisotropic. In order to check the degree of orientation, azimuthal integration of this peak was made (Figure 6). The peaks widths of normalized intensity are the same, which indicates that certain PCL matrix orientation is similar in all samples. This means that PCL crystalline structure is not affected by the PLA fibrils.

All the diffractograms in Figure 7 are similar with the same peaks positions and intensities. One minor deviation can be observed for the PLA (200) peak. It seems that the incorporation of higher content (5%) of halloysite reduces PLA crystallinity. This makes very small impact on overall crystallinity which is around 51%.

In Figure 8, one can see formed PCL lamellar stacks as a peak at $q$ = 0.04 Å$^{-1}$ [50]. For the scattering

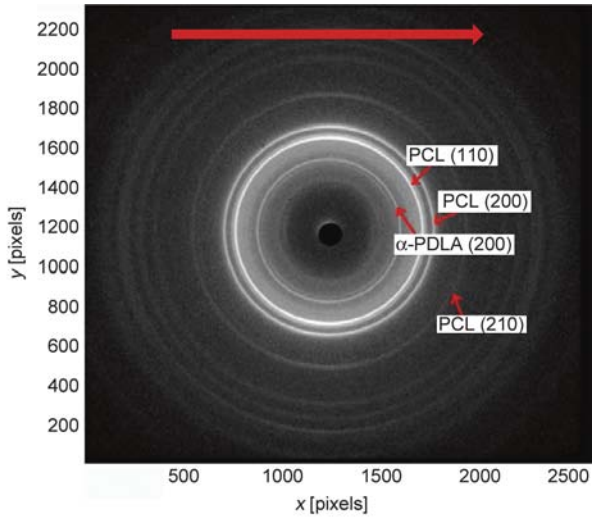


**Figure 5.** 2D WAXS for the undrawn PCL/PLA sample 80/20. Arrow showing the flow (injection moulding) direction.

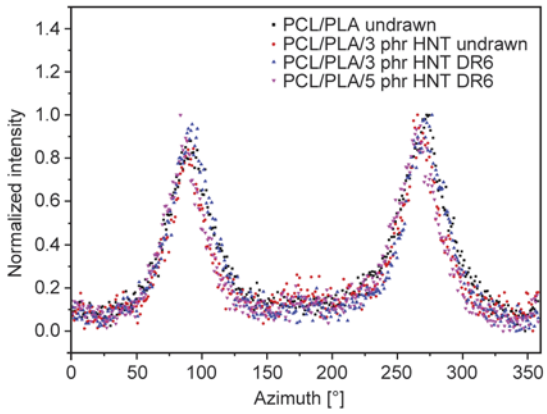


**Figure 6.** Azimuthal averaging of PCL (110) peak

curves corresponding to PCL/PLA with halloysite, the intensity falls with the slope $q^{-1.8}$ at lower angles. This is in agreement with tubular structure of HNT [51]. For these samples, the lamellar peak is overlapped by strong signal corresponding to halloysite. The presence of small bump at $q$ = 0.021 Å$^{-1}$ is given by the diameter of halloysite (~300 Å$^{-1}$). Small changes at higher $q$-values are given by the degree of tubes filling. With higher amount of HNT, the average amount of material inside the tubes is lower, which lowers the overall intensity. For the drawn sample PCL/PLA/HNT 80/20/3, the drawing increases intensity, which indicates possible higher incorporation of polymer into the lumen of halloysite tubes.

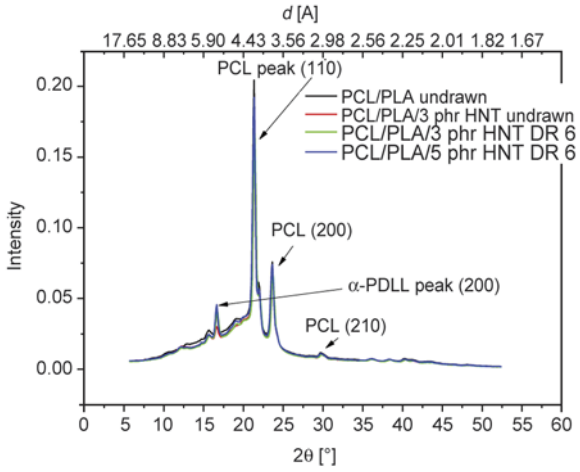


**Figure 7.** Effect of HNT and drawing on diffractograms

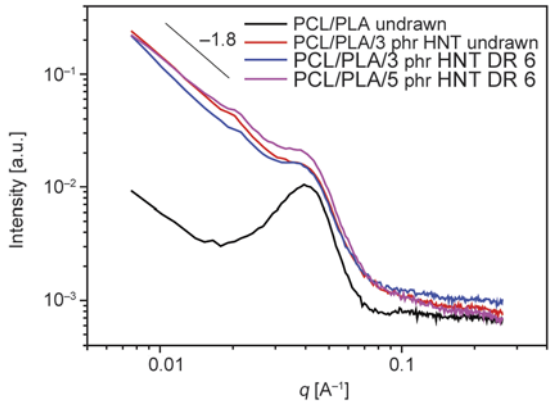


**Figure 8.** One-dimensional SAXS patterns

*Differential scanning calorimetry*

Typical DSC thermogram of the studied PCL/PLA/HNT 80/20/3 system is shown in Figure 9. PCL and PLA show maximum of the melting endotherm at about 62 and 151 °C, respectively. The glass transition temperature of PLA (about 61 °C) is hidden under the PCL endotherm. A flat exotherm appears between the two melting endotherms. It belongs to cold crystallization of PLA that crystallizes after crossing $T_g$. This exotherm provides the value $CR_c$ in Table 2 that should be subtracted from the total crystallinity $CR_m$ to receive PLA crystallinity of the as-prepared samples $CR_p$.

Table 2 shows that melting temperatures (i.e. measures of crystal perfection) of both PCL and PLA do not show any significant dependence either on added filler, drawing or processing temperature. This finding corresponds to the WAXS observations. Neat

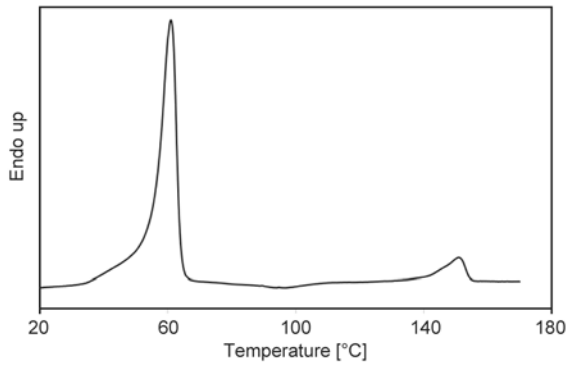


**Figure 9.** DSC thermogram of PCL/PLA/HNT 80/20/3

**Table 2.** DSC results of PCL, PLA, their blends (80/20) and microfibrillar composites. Melting temperature $T_m$, crystallinity $CR$. For $CR$ of PLA the subscripts mean: $c$ – cold crystallization, $m$ – final melting, $p$ – as-prepared

| Sample | DR | Process temperature [°C] | PCL | | PLA | | | |
|---|---|---|---|---|---|---|---|---|
| | | | $T_m$ [°C] | $CR$ [%] | $CR_c$ [%] | $T_m$ [°C] | $CR_m$ [%] | $CR_p$ [%] |
| PCL | 1 | 137 | 63.2 | 53.6 | – | – | – | – |
| PLA | 1 | 190 | – | – | 6.5 | 151.1 | 8.1 | 1.6 |
| PLA, 70°C, 60 min | 1 | 190 | – | – | 0.5 | 151.7 | 29.3 | 28.8 |
| PLA 1% HNT, 70 °C, 60 min | 1 | 190 | – | – | 0.5 | 154.4 | 32.7 | 32.2 |
| PCL/PLA 80/20 | 1 | 137 | 62.8 | 52.0 | 5.8 | 150.7 | 32.6 | 26.8 |
| PCL/PLA/HNT 80/20/3 | 1 | 137 | 63.5 | 48.8 | 9.1 | 152.3 | 40.7 | 31.6 |
| PCL/PLA/HNT 80/20/3 | 6 | 137 | 62.8 | 51.3 | 5.6 | 151.3 | 40.2 | 35.9 |
| PCL/PLA/HNT 80/20/5 | 6 | 137 | 61.5 | 48.2 | 1.5 | 149.5 | 20.3 | 18.8 |
| PCL/PLA/HNT 80/20/3 | 1 | 200 | 61.0 | 51.4 | 18.9 | 150.9 | 34.9 | 16.0 |
| PCL/PLA/HNT 80/20/3 | 6 | 200 | 60.6 | 47.9 | 20.0 | 151.6 | 34.0 | 14.0 |

PLA is almost amorphous as demonstrated by the very low value (1.6 phr) of $CR_p$. However, its crystallinity dramatically increases on blending with PCL [4] and subsequent annealing of the samples during the process of injection moulding at 137 °C for ~4 min accompanied by PLA cold crystallization. Optimum filler concentration seems to be 3 phr. Another increase in PLA crystallinity to ~36% is achieved by MFC formation by drawing, probably as a consequence of chain orientation in the fibrils. Higher filler concentration (5 phr) leads to lower crystallinity in accordance with the WAXS results. It seems that in this case hindering effect of the filler takes place, which leads to limited growth of spherulites. At high processing temperature (200 °C), the PLA phase including fibrils melts, which has a negative effect on PLA crystallinity. This documents the importance of PLA annealing below its melting point. This effect is particularly apparent for the samples of neat PLA and the PLA/HNT composite annealed at 70 °C. In both cases, the as-prepared samples show high crystallinity $CR_p$ of about 30% and negligible cold crystallization.

### 3.4. Effect of HNT and drawing on mechanical properties

The data are summarized in Table 3. Blending (PCL/PLA 80/20) results in increased yield stress $\sigma_y$ and modulus $E$ in comparison with the PCL matrix. On the other hand, unchanged $\sigma_m$ and significantly reduced $\varepsilon_b$ and at indicate reduced ductility of PCL by addition of rigid PLA. These trends are more intensive on addition of HNT – small increase in yield stress and modulus is accompanied by significantly reduced strain hardening, as also shown in Figure 10.

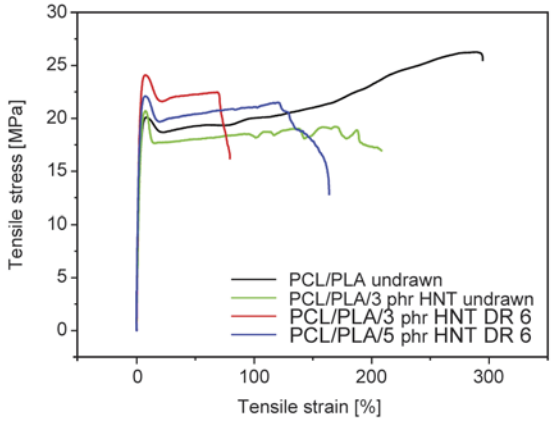


**Figure 10.** Stress-strain curves of PCL/PLA 80/20 blend and related MFC containing HNT

The best mechanical behaviour, i.e. particularly yield stress and modulus, was found for the one-step prepared PCL/PLA 80/20 sample with 3 phr HNT drawn at DR = 6. This corresponds to the fibril formation only possible after the modification of the PCL/PLA system by HNT (see above). The fair mechanical performance of this biodegradable PCL-based material (MFC) is predominantly a consequence of the dual reinforcement by PLA fibrils of AR ~12 and HNT. In addition, the increase in PLA crystallinity to about 30% as a result of 'annealing' in the course of sample injection moulding at 137°C (see Table 2) leading to improvement of mechanical parameters of the PLA component is also important (Table 3). This was confirmed by testing neat PLA and PLA + 1% HNT prepared by injection mould-

**Table 3.** Mechanical properties of components, PCL/PLA 80/20 blend, and MFC in dependence on HNT content. Pre-blended components are in brackets.

| Sample composition | DR | $\sigma_y$ [MPa] | $\sigma_m$ [MPa] | $\varepsilon_y$ [%] | $\varepsilon_b$ [%] | $E$ [MPa] | [kJ/m$^2$] |
|---|---|---|---|---|---|---|---|
| PCL | 1 | 16.10 | 27.00 | 9.4 | 472.00 | 310 | 85.4 |
| PCL 3% HNT | 1 | 15.90 | 31.70 | 8.6 | 705.00 | 420 | 59.0 |
| PLA | 1 | 68.00 | 68.00 | 2.7 | 4.30 | 3155 | 18.9 |
| PLA 1% HNT | 1 | 66.80 | 58.00 | 2.3 | 4.00 | 3310 | – |
| PLA 3% HNT | 1 | 62.70 | 53.00 | 2.0 | 6.00 | 3480 | 24.2 |
| PLA 70 °C[a] | 1 | 69.70 | 69.70 | 3.1 | 4.05 | 3860 | – |
| PLA 1% HNT 70 °C[a] | 1 | 68.20 | 54.00 | 4.6 | 4.60 | 4155 | – |
| PCL/PLA 80/20 | 1 | 20.20 | 26.80 | 7.6 | 295.00 | 720 | 60.8 |
| PCL/PLA/HNT 80/20/3 | 1 | 20.80 | 20.80 | 7.8 | 201.00 | 795 | 34.0 |
| PCL/PLA/HNT 80/20/3 | 6 | 23.85 | 23.85 | 7.1 | 83.00 | 985 | 38.6 |
| PCL/PLA/HNT 80/20/5 | 6 | 22.00 | 22.40 | 7.6 | 143.00 | 945 | 49.7 |
| (PCL+3% HNT)[b]/PLA 80/20 | 5 | 21.40 | 27.00 | 9.7 | 374.00 | 905 | – |
| PCL/(PLA+3% HNT)[c]/HNT 80/20/3 | 1 | 20.90 | 14.00 | 8.1 | 548.00 | 820 | 35.2 |
| PCL/(PLA+3% HNT)[c]/HNT 80/20/3 | 5 | 22.60 | 12.60 | 7.6 | 120.00 | 935 | 45.4 |

[a]annealed 60 min at 70 °C, [b]pre-blend PLA/1% C15, [c]pre-blend PCL/3% C15

ing at 190 °C and subsequent annealing at 70 °C for 1 h. These samples show crystallinities of about 30% (Table 2) and approximate 20% increase in modulus (Table 3).

Surprisingly, increasing the HNT content from 3 to 5 phr in MFC results in reduced yield strength and modulus whereas toughness and elongation are higher, which is quite an unusual result. This can be partially attributed to the lower crystallinity of PLA in MFC with 5 phr HNT (see Table 2), but predominantly to the complex effect of HNT, including changes in the interface [52]. Such effect was also found in the analogous oMMT-modified systems [40].

Table 3 also shows that pre-blending of HNT in PCL is less effective in comparison with the one-step preparation, contrary to the analogous clay–modified system [40]. Reduction in yield stress and modulus is accompanied by more significant strain hardening.

The application of PLA/HNT pre-blend does not lead to MFC formation due to the impossibility of drawing. Drawing is enabled by the simultaneous addition of 3 phr HNT, similarly to the oMMT-modified system [40]. The importance of the mixing protocol also indicates crucial role of the nanofiller transfer between the polymer components in the course of drawing [42]. This may lead to changed HNT arrangement and its localization in the interfacial area. This could change crystallinity and thus parameters of the interface that would result in modified properties of the whole system [52].

Undoubtedly, mechanical properties can also be affected by HNT localization in the respective polymer phases and is related to different degrees of their reinforcement. TEM observations (Figure 3) show relatively low content of HNT inside PLA and its more significant localization in PCL. Unfortunately, exact content of HNT in the respective components cannot be determined as their separation is impossible. Regarding the effect of HNT localization on mechanical behaviour, it is apparent that its increased content in one component at the expense of the other may affect properties due to uneven ratio of the components.

An example is a model PCL/PLA 80/20 system with 1% HNT in the PLA phase and 3% HNT in PCL. For the 0.25% increase of HNT in PCL by transfer of 1% from PLA (and resulting in changes of $E$, assuming linear dependence of $E$ on HNT content) and the opposite case of similar transfer of 0.25% from PCL to PLA, the Halpin-Tsai model [53] shows difference in $E$ between both cases of ~30 MPa only. This implies that HNT reinforcement of the system is particularly important, whereas its localization in the respective polymer phases has relatively low impact.

The properties of HNT-modified MFCs are comparable and some of their parameters even exceed those of the analogous oMMT-modified system (of similar AR of fibrils) [40]. The fact that such behaviour has been found in spite of the lower reinforcing effect of HNT on the neat components in comparison with oMMT also confirms the complex effect of both nanofillers.

Significant difference from oMMT-modified MFC is very low strain hardening or its practical absence in HNT-containing MFC shown in Table 3 and Figure 10. This tensile behaviour occurs already in the undrawn HNT-containing sample probably as a consequence of the above mentioned increased PLA crystallinity caused by annealing during injection moulding below the melting point of PLA. In the drawn system, the post-yield drawing is suppressed more markedly by the presence of the PLA fibrils. Moreover, this occurs in spite of similar extent of elongation ($\varepsilon_b$) of both MFCs. Such behaviour is also significantly different from that of the PCL/HNT and undrawn PCL/PLA systems (Table 3), where stress at break exceeds the value of 30 and 27 MPa, respectively.

### 3.5. Effect of HNT on rheology of components and MFC

As mentioned above, TEM (Figure 3) indicates the localization of HNT in the PCL and PLA phases and at the interface, with predominant occurrence in the PCL matrix. The presence of HNT leads to remarkable increase in viscosity of PCL, PLA, and the PCL/PLA blend (see Figure 11). The changed rheological behaviour, including the effect of orientation of anisotropic HNT at higher shear rates, is apparently responsible for increased stability of extrusion rendering the cold drawing possible. The difference in rheological properties of the drawn and undrawn PCL/PLA/HNT nanocomposites (see Figure 12), measured at 137 °C to avoid melting of the PLA fibrils, can be explained as a consequence of presence of the PLA fibrils in the first system in comparison with spherical inclusions in the other. It can be assumed that the orientation of the PLA

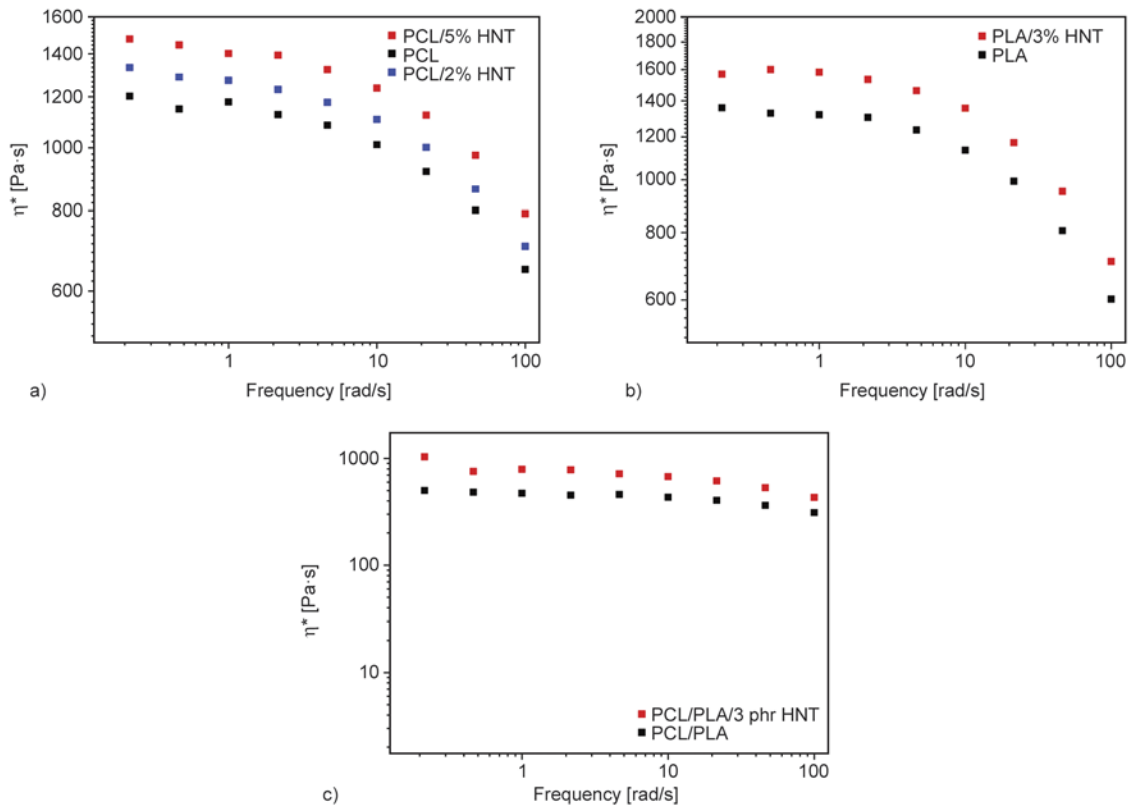


**Figure 11.** Effect of HNT addition on complex viscosity of a) PCL, b) PLA, c) PCL/PLA 80/20 system at 170 °C

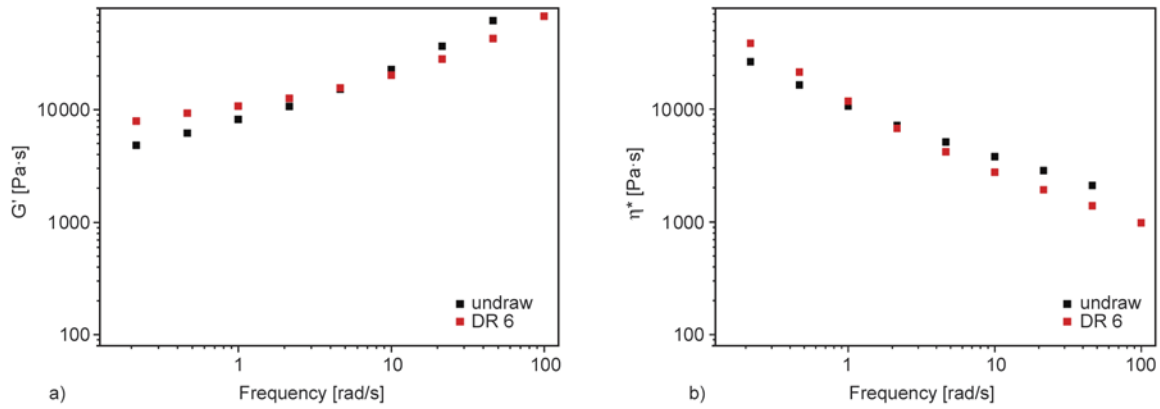


**Figure 12.** Effect of HNT addition on a) storage modulus and b) complex viscosity of undrawn and melt drawn PCL/PLA/HNT 80/20/3 systems at 137 °C

fibres disappears to a large extent during preparation of the specimens for rheological measurements and melting of the PCL matrix before start of the measurements.

For a certain volume fraction of dispersed particles, percolation threshold in the system and distance between a particle and its nearest neighbour decrease with increasing particle anisometry. Therefore, stronger interactions can be assumed for a system with more anisometric particles which increase viscosity and storage modulus of the system measured at low frequencies. On the other hand, more anisometric particles are more easily oriented in flow, which explains faster decrease in viscosity and storage modulus with increasing angular frequency. In other words, the rheological behaviour of MFC is typical of short fibre composites [54]. At the same time, the rather small difference in η* and *G* between undrawn blend and MFC is a result of certain presence of apparently anisometric PLA particles caused by flow in the extruder die [42].

## 4. Conclusions

The results obtained indicate a complex effect of HNT on the behaviour of the PCL /PLA microfibrillar composite. This is mainly reflected by the modification of the rheological parameters of the polymer components leading to stable extrusion and thus melt drawing which is impossible in the HNT-free blend. Although further important effect of HNT is reinforcement of the polymer components, the best performance with low 3 phr HNT content indicates important role of HNT-induced effects on, e.g., interface and fibrils parameters affecting deformational behaviour. The final MFC processing below the melting point of PLA leads to favourable increase in crystallinity of nearly amorphous neat PLA and enhanced mechanical performance. As a result, the material with the biodegradable PCL matrix of significantly improved mechanical behaviour is obtained.

## Acknowledgements

This work was supported by Czech Science Foundation (Grant No 13-15255S).

## References

[1] Woodruff M. A., Hutmacher D. W.: The return of a forgotten polymer – Polycaprolactone in the 21st century. Progress in Polymer Science, **35**, 1217–11256 (2010). DOI: 10.1016/j.progpolymsci.2010.04.002

[2] Simões C. L., Viana J. C., Cunha A. M.: Mechanical properties of poly(ε-caprolactone) and poly(lactic acid) blends. Journal of Applied Polymer Science, **112**, 345–352 (2009). DOI: 10.1002/app.29425

[3] Yeh J-T., Wu C-J., Tsou C-H., Chai W-L., Chow J-D., Huang C-J., Chen K-N., Wu C-S.: Study on the crystallization, miscibility, morphology, properties of poly(lactic acid)/poly(ε-caprolactone) blends. Polymer-Plastics Technology and Engineering, **48**, 571–578 (2009). DOI: 10.1080/03602550902824390

[4] Urquijo J., Guerrica-Echevarría G., Eguiazábal J. I.: Melt processed PLA/PCL blends: Effect of processing method on phase structure, morphology, and mechanical properties. Journal of Applied Polymer Science, **132**, 42641/1–42641/9 (2015). DOI: 10.1002/app.42641

[5] López-Rodríguez N., López-Arraiza A., Meaurio E., Sarasua J. R.: Crystallization, morphology, and mechanical behavior of polylactide/poly(ε-caprolactone) blends. Polymer Engineering and Science, **46**, 1299–1308 (2006). DOI: 10.1002/pen.20609

[6] Na Y-H., He Y., Shuai X., Kikkawa Y., Doi Y., Inoue Y.: Compatibilization effect of poly(ε-caprolactone)-*b*-poly(ethylene glycol) block copolymers and phase morphology analysis in immiscible poly(lactide)/poly (ε-caprolactone) blends. Biomacromolecules, **3**, 1179–1186 (2002). DOI: 10.1021/bm020050r

[7] Tuba F., Oláh L., Nagy P.: Characterization of reactively compatibilized poly(D,L-lactide)/poly(ε-caprolactone) biodegradable blends by essential work of fracture method. Engineering Fracture Mechanics, **78**, 3123–3133 (2011). DOI: 10.1016/j.engfracmech.2011.09.010

[8] Jain S., Reddy M. M., Mohanty A. K., Misra M., Ghosh A. K.: A new biodegradable flexible composite sheet from poly(lactic acid)/poly(ε-caprolactone) blends and micro-talc. Macromolecular Materials and Engineering, **295**, 750–762 (2010). DOI: 10.1002/mame.201000063

[9] Wu D., Lin D., Zhang J., Zhou W., Zhang M., Zhang Y., Wang D., Lin B.: Selective localization of nanofillers: Effect on morphology and crystallization of PLA/PCL blends. Macromolecular Chemistry and Physics, **212**, 613–626 (2011). DOI: 10.1002/macp.201000579

[10] Hasook A., Tanoue S., Iemoto Y., Unryu T.: Characterization and mechanical properties of poly(lactic acid)/poly(ε-caprolactone)/organoclay nanocomposites prepared by melt compounding. Polymer Engineering and Science, **46**, 1001–1007 (2006). DOI: 10.1002/pen.20579

[11] Li Q., Yoon J-S., Chen G-X.: Thermal and biodegradable properties of poly(L-lactide)/poly(ε-caprolactone) compounded with functionalized organoclay. Journal of Polymers and the Environment, **19**, 59–68 (2011). DOI: 10.1007/s10924-010-0256-2

[12] Goffin A-L., Habibi Y., Raquez J-M., Dubois P.: Polyester-grafted cellulose nanowhiskers: A new approach for tuning the microstructure of immiscible polyester blends. ACS Applied Materials and Interfaces, **4**, 3364–3371 (2012). DOI: 10.1021/am3008196

[13] Kaygusuz I., Kaynak C.: Influences of halloysite nanotubes on crystallisation behaviour of polylactide. Plastics, Rubber and Composites, Macromolecular Engineering, **44**, 41–49 (2015). DOI: 10.1179/1743289814Y.0000000116

[14] Liu M., Zhang Y., Zhou C.: Nanocomposites of halloysite and polylactide. Applied Clay Science, **75–76**, 52–59 (2013). DOI: 10.1016/j.clay.2013.02.019

[15] Lee K-S., Chang Y-W.: Thermal, mechanical, and rheological properties of poly(ε-caprolactone)/halloysite nanotube nanocomposites. Journal of Applied Polymer Science, **128**, 2807–2816 (2013). DOI: 10.1002/app.38457

[16] Khunová V., Kelnar I., Kristóf J., Dybal J., Kratochvíl J., Kaprálková L.: The effect of urea and urea-modified halloysite on performance of PCL. Journal of Thermal Analysis and Calorimetry, **120**, 1283–1291 (2015). DOI: 10.1007/s10973-015-4448-9

[17] Pasbakhsh P., Ismail H., Ahmad Fauzi M. N., Abu Bakar A.: EPDM/modified halloysite nanocomposites. Applied Clay Science, **48**, 405–413 (2010). DOI: 10.1016/j.clay.2010.01.015

[18] Khunova V., Kristóf J., Kelnar I., Dybal J.: The effect of halloysite modification combined with *in situ* matrix modifications on the structure and properties of polypropylene/halloysite nanocomposites. Express Polymer Letters, **7**, 471–479 (2013). DOI: 10.3144/expresspolymlett.2013.43

[19] Pal P., Kundu M. K., Kalra S., Das C. K.: Mechanical and crystalline behavior of polymeric nanocomposites in presence of natural clay. Open Journal of Applied Sciences, **2**, 277–282 (2012). DOI: 10.4236/ojapps.2012.24041

[20] Poikelispää M., Das A., Dierkes W., Vuorinen J.: Synergistic effect of plasma-modified halloysite nanotubes and carbon black in natural rubber–butadiene rubber blend. Journal of Applied Polymer Science, **127**, 4688–4696 (2013). DOI: 10.1002/app.38080

[21] Pal P., Kundu M. K., Malas A., Das C.: Compatibilizing effect of halloysite nanotubes in polar–nonpolar hybrid system. Journal of Applied Polymer Science, **131**, 39587/1–39587/7 (2014). DOI: 10.1002/app.39587

[22] Russo P., Vetrano B., Acierno D., Mauro M.: Thermal and structural characterization of biodegradable blends filled with halloysite nanotubes. Polymer Composites, **34**, 1460–1470 (2013). DOI: 10.1002/pc.22419

[23] Tham W. L., Mohd Ishak Z. A., Chow W. S.: Mechanical and thermal properties enhancement of poly(lactic acid)/halloysite nanocomposites by maleic-anhydride functionalized rubber. Journal of Macromolecular Science Part B: Physics, **53**, 371–382 (2014). DOI: 10.1080/00222348.2013.839314

[24] Gelfer M. Y., Song H. H., Liu L., Hsiao B. S., Chu B., Rafailovich M., Si M., Zaitsev V.: Effects of organoclays on morphology and thermal and rheological properties of polystyrene and poly(methyl methacrylate) blends. Journal of Polymer Science Part B: Polymer Physics, **41**, 44–54 (2003). DOI: 10.1002/polb.10360

[25] Rotrekl J., Matějka L., Kaprálková L., Zhigunov A., Hromádková J., Kelnar I.: Epoxy/PCL nanocomposites: Effect of layered silicate on structure and behavior. Express Polymer Letters, **6**, 975–986 (2012). DOI: 10.3144/expresspolymlett.2012.103

[26] Kelnar I., Sukhanov V., Rotrekl J., Kaprálková L.: Toughening of recycled poly(ethylene terephthalate) with clay-compatibilized rubber phase. Journal of Applied Polymer Science, **116**, 3621–3628 (2010). DOI: 10.1002/app.31905

[27] Kelnar I., Rotrekl J., Kaprálková L., Hromádková J., Strachota A.: Effect of amine-terminated butadiene-acrylonitrile/clay combinations on the structure and properties of epoxy nanocomposites. Journal of Applied Polymer Science, **125**, 3477–3483 (2012). DOI: 10.1002/app.36696

[28] Ju D., Han L., Li F., Chen S., Dong L.: Crystallization, mechanical properties, and enzymatic degradation of biodegradable poly(ε-caprolactone) composites with poly(lactic acid) fibers. Polymer Composites, **34**, 1745–1752 (2013). DOI: 10.1002/pc.22578

[29] Neppalli R., Marega C., Marigo A., Bajgai M. P., Kim H. Y., Causin V.: Improvement of tensile properties and tuning of the biodegradation behavior of polycaprolactone by addition of electrospun fibers. Polymer, **52**, 4054–4060 (2011). DOI: 10.1016/j.polymer.2011.06.039

[30] Chen J., Lu L., Wu D., Yuan L., Zhang M., Hua J., Xu J.: Green poly(ε-caprolactone) composites reinforced with electrospun polylactide/poly(ε-caprolactone) blend fiber mats. ACS Sustainable Chemistry and Engineering, **2**, 2102–2110 (2014). DOI: 10.1021/sc500344n

[31] Fakirov S., Bhattacharyya D., Shields R. J.: Nanofibril reinforced composites from polymer blends. Colloids and Surfaces A: Physicochemical and Engineering Aspects, **313**, 2–8 (2008.) DOI: 10.1016/j.colsurfa.2007.05.038

[32] Dencheva N., Oliveira M. J., Carneiro O. S., Pouzada A. S., Denchev Z.: Preparation, structural development, and mechanical properties of microfibrillar composite materials based on polyethylene/polyamide 6 oriented blends. Journal of Applied Polymer Science, **115**, 2918–2932 (2010). DOI: 10.1002/app.31389

[33] Li Z-M., Li L-B., Shen K-Z., Yang W., Huang R., Yang M-B.: Transcrystalline morphology of an *in situ* microfibrillar poly(ethylene terephthalate)/poly(propylene) blend fabricated through a slit extrusion hot stretching-quenching process. Macromolecular Rapid Communications, **25**, 553–558 (2004). DOI: 10.1002/marc.200300086

[34] Friedrich K., Hoffmann J., Evstatiev M., Ye L., Mai Y. W.: Improvements of stiffness and strength of bioresorbable bone nails by the MFC-concept. Key Engineering Materials, **334–335**, 1181–1184 (2007). DOI: 10.4028/www.scientific.net/KEM.334-335.1181

[35] Kimble L. D., Bhattacharyya D., Fakirov S.: Biodegradable microfibrillar polymer-polymer composites from poly(L-lactic acid)/poly(glycolic acid). Express Polymer Letters, **9**, 300–304 (2015).
DOI: 10.3144/expresspolymlett.2015.27

[36] Xie L., Xu H., Niu B., Ji X., Chen J., Li Z-M., Hsiao B. S., Zhong G-J.: Unprecedented access to strong and ductile poly(lactic acid) by introducing *in situ* nanofibrillar poly(butylene succinate) for green packaging. Biomacromolecules, **15**, 4054–5064 (2014).
DOI: 10.1021/bm5010993

[37] Simeonova S., Evstatiev M., Li W., Burkhart T.: Fabrication and characterization of biodegradable polymer scaffolds adapting microfibrillar composite concept. Journal of Polymer Science Part B: Polymer Physics, **51**, 1298–1310 (2013).
DOI: 10.1002/polb.23332

[38] Haroosh H. J., Dong Y., Chaudhary D. S., Ingram G. D., Yusa S-I.: Electrospun PLA: PCL composites embedded with unmodified and 3-aminopropyltriethoxysilane (ASP) modified halloysite nanotubes (HNT). Applied Physics A: Materials Science and Processing, **110**, 433–442 (2013).
DOI: 10.1007/s00339-012-7233-7

[39] Lu L., Wu D., Zhang M., Zhou W.: Fabrication of polylactide/poly(ε-caprolactone) blend fibers by electrospinning: Morphology and orientation. Industrial and Engineering Chemistry Research, **51**, 3682–3691 (2012).
DOI: 10.1021/ie2028969

[40] Kelnar I., Fortelný I., Kaprálková L., Kratochvíl J., Angelov B., Nevoralová M.: Effect of layered silicates on fibril formation and properties of PCL/PLA microfibrillar composites. Journal of Applied Polymer Science, **133**, 43061/1–43061/9 (2015).
DOI: 10.1002/app.43061

[41] Shields R. J., Bhattacharyya D., Fakirov S.: Fibrillar polymer–polymer composites: Morphology, properties and applications. Journal of Materials Science, **43**, 6758–6770 (2008).
DOI: 10.1007/s10853-008-2693-z

[42] Kelnar I., Kaprálková L., Kratochvíl J., Kotek J., Kobera L., Rotrekl J., Hromádková J.: Effect of nanofiller on the behavior of a melt-drawn HDPE/PA6 microfibrillar composite. Journal of Applied Polymer Science, **132**, 41868/1–41868/9 (2015).
DOI: 10.1002/app.41868

[43] Wojdyr M.: Fityk: A general-purpose peak fitting program. Journal of Applied Crystallography, **43**, 1126–1128 (2010).
DOI: 10.1107/S0021889810030499

[44] Fakirov S., Bhattacharyya D., Lin R. J. T., Fuchs C., Friedrich K.: Contribution of coalescence to microfibril formation in polymer blends during cold drawing. Journal of Macromolecular Science Part B: Physics, **46**, 183, 193 (2007).
DOI: 10.1080/00222340601044375

[45] Kelnar I., Fortelný I., Kaprálková L., Hromádková J.: Effect of nanofiller on fibril formation in melt-drawn HDPE/PA6 microfibrillar composite. Polymer Engineering and Science, **55**, 2133–2139 (2015).
DOI: 10.1002/pen.24055

[46] Filippone G., Acierno D.: Clustering of coated droplets in clay-filled polymer blends. Macromolecular Materials and Engineering, **297**, 923–928 (2012).
DOI: 10.1002/mame.201100398

[47] Brus J., Urbanová M., Kelnar I., Kotek J.: A solid-state NMR study of structure and segmental dynamics of semicrystalline elastomer-toughened nanocomposites. Macromolecules, **39**, 5400–5409 (2006).
DOI: 10.1021/ma0604946

[48] Coativy G., Chevigny C., Rolland-Sabaté A., Leroy E., Lourdin D.: Interphase vs confinement in starch-clay bionanocomposites. Carbohydrate Polymers, **117**, 746–752 (2015).
DOI: 10.1016/j.carbpol.2014.10.052

[49] Moll J., Kumar S. K.: Glass transitions in highly attractive highly filled polymer nanocomposites. Macromolecules, **45**, 1131–1135 (2012).
DOI: 10.1021/ma202218x

[50] Chuang W-T., Jeng U-S., Hong P-D., Sheu H-S., Lai Y-H., Shih K-S.: Dynamic interplay between phase separation and crystallization in a poly(ε-caprolactone)/poly(ethylene glycol) oligomer blend. Polymer, **48**, 2919–2927 (2007).
DOI: 10.1016/j.polymer.2007.03.041

[51] Kamble R., Ghag M., Gaikawad S., Panda B. K.: Halloysite nanotubes and applications: A review. Journal of Advanced Scientific Research, **3**, 25–29 (2012).

[52] Kelnar I., Kaprálková L., Kratochvíl J., Padovec Z., Růžička M., Hromádková J.: Effect of layered silicates and reactive compatibilization on structure and properties of melt-drawn HDPE/PA6 microfibrillar composites. Polymer Bulletin, in press (2016).
DOI: 10.1007/s00289-015-1570-6

[53] Halpin J. C., Kardos J. L.: The Halpin-Tsai equations: A review. Polymer Engineering and Science, **16**, 344–352 (1976).
DOI: 10.1002/pen.760160512

[54] Vinogradov G. V., Malkin A. Y.: Rheology of polymers. Mir Publishers, Moscow (1980).